Chapter 2

The Yellow Sea Surface Cold Patches in Warm Seasons

X. San Liang, Minghai Huang, Hui Wu and Yihe Wang

Additional information is available at the end of the chapter

http://dx.doi.org/10.5772/intechopen.80732

Abstract

An important hydrographic phenomenon in the Yellow Sea is the surface cold patches (SCP) in warm seasons, among which the most conspicuous are the Shandong SCP, Subei SCP, and Mokpo SCP. Previous studies based on monthly mean fields propose that these patches result from the collaboration of tidal mixing and tidal induced upwelling. While this is true for patches like the Shandong SCP, the monthly mean tidal mixing and upwelling alone cannot explain all their formations. In this study, through a detailed analysis of their patterns over a spring-neap tidal cycle, it is found that the Subei and Mokpo SCPs show distinct spring-neap variations. During the neap tide phase, strong stratification is established, and hence the cold patches in these two areas may be greatly weakened or even suppressed, while during the spring tide phase, the surface temperature reaches its minimum. That is to say, for these two SCPs, besides the well-accepted mechanisms, the effect of spring-neap tidal variation must be taken into account.

Keywords: Yellow Sea, upwelling, tidal mixing, surface cold patches

1. Introduction

The Yellow Sea is the northern part of the East China Sea, a western Pacific marginal shallow sea surrounded by China and Korea (**Figure 1**). Approximately, it has a meridional extension of 960 km, a zonal extension of 700 km, and an average depth of 44 m, with a maximum of 100 m in the central trough. Its sea bottom and shores are full of sand and silt carried by the Yellow River (Huanghe) and other rivers. These deposits, together with the sand storms from the Gobi Desert, turn the surface of the water golden yellow, making it one of the four seas named after color—the others being the Black Sea between Eastern Europe and Western Asia, the Red Sea near Gulfs of Aden and Suez, and the White Sea on the northwest coast of Russia.

IntechOpen

© 2018 The Author(s). Licensee IntechOpen. Distributed under the terms of the Creative Commons Attribution-NonCommercial 4.0 License (https://creativecommons.org/licenses/by-nc/4.0/), which permits use, distribution and reproduction for non-commercial purposes, provided the original is properly cited.

BY-NC

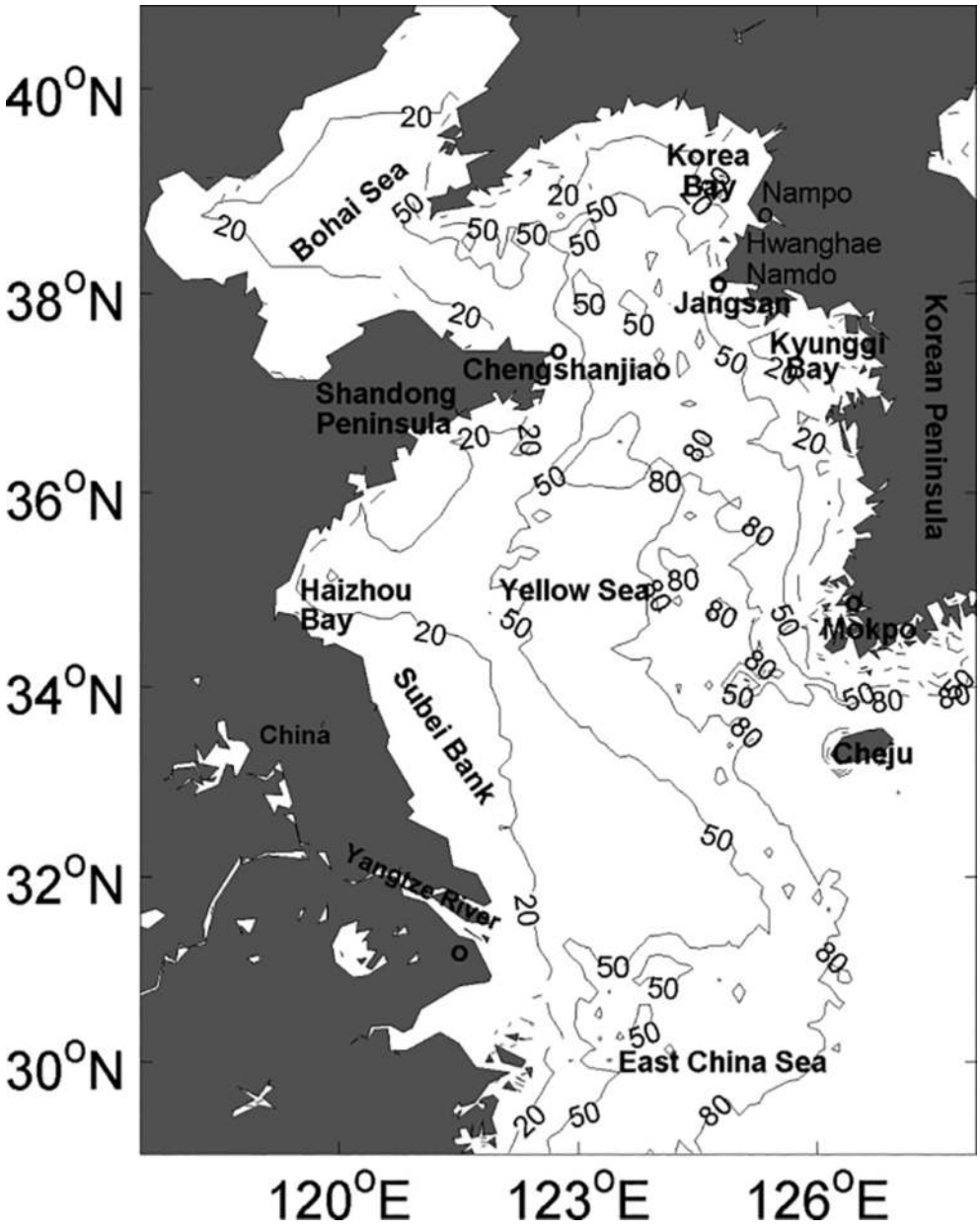

Figure 1. Bathymetry of the study area (contour interval: 30 m).

It has long been observed that cold water masses prevail in warm seasons in the deep or bottom layers of the central Yellow Sea. These are the Yellow Sea Cold Water Mass (YSCWM), a conspicuous phenomenon which has attracted wide attention from physical oceanographers

ever since 1921 [1]. YSCWM is induced by bottom topography and summer atmospheric conditions. It has a double-cell circulation. It is believed to have a double-cell circulation. The detailed circulation, however, is still controversial. Proposed so far are three structures: (1) above the thermocline, it is an anticyclonic horizontal circulation with downwelling at the center and upwelling around; below the thermocline the circulation is the opposite [2]; (2) the double cell is formed by convection, with upwelling at the center through the whole water column and downwelling near the coast [3]. But the convection is limited within a thin shell, outside which the water is almost motionless in the vertical direction; and (3) based on the observations and numerical modeling, Su and Huang [4] found a structure similar to (1), but with totally opposite flow directions. That is to say, it is a cyclonic flow above and an anticyclonic flow below, with the accordingly vertical circulations. All these, however, are yet to be verified with more observations.

Around the YSCWM, we often observe cold centers at the sea surface (e.g., [5, 6]), in contrast to the ambient high SST in boreal summer. These are the surface cold patches (SCPs). For the SCPs off Mokpo, Korea, their generation has been ascribed to tidal mixing (e.g., [7]). But details are yet to be revealed. Recently, Lu et al. [8] reported that tidal mixing and tide-induced upwelling may collaborate to lead to the formation of the SCPSs. By observation, the patches sit along the slope of the Yellow Sea trough, where intensified tidal mixing occurs. The abrupt change of bathymetry tends to increase the velocity shear and hence enhance the vertical mixing, while the enhanced mixing will change the horizontal density distribution, leading to a secondary upwelling. This is further substantiated by the observation that the SCP sites agree with the occurrences of maximal tidal currents, which result in extensive tidal mixing and, by the above argument, strong upwelling (cf. Figure 12 in [8]).

The generating mechanism via tidal mixing implies that there must be a good correspondence [8, 9] between the SCP locations and the Simpson-Hunter index [10],

$$\mathrm{SH} = \log\left(\mathrm{H}/|\mathrm{U}^3|\right), \tag{1}$$

(where H and U are, respectively, the water depth and the amplitude of the tidal velocity), which describes, for the summer shelf seas, the influence of surface buoyancy input and tidal mixing in controlling the water column structure. By the SH distribution, there are three conspicuous fronts in the Yellow Sea; they are, in a clockwise order, Subei Bank Front (SBF), Shandong Peninsula Front (SPF), and Mokpo Front (MKF) [11]. Correspondingly, three most conspicuous SCPs are identified. Through comparative experiments, it is found that the SCPs off Shandong and Mokpo are mainly induced, respectively, through tidal mixing and tide-induced upwelling, while the Subei SCP is generated through a combination of the two mechanisms. In a word, tidal mixing and tide-induced upwelling are the two key factors in the formation of the SCPs.

The above analyses are with the monthly mean maps of the summer sea surface temperature (SST). However, by observation, the SCPs actually do not last throughout the summer; they sometimes disappear. A monthly mean analysis may exclude some possible mechanism(s) in arriving at the mean fields. In fact, we do see such an example in Chesapeake Bay, where the spring-neap tidal cycles are found to exert effects on the turbulent mixing, stratification, and residual circulation [12]. For the Yellow Sea (and the surrounding seas like Bohai Sea and East

Sea), satellite ocean color observations have also shown distinct difference of ocean optical and biogeochemical properties over a spring-neap tidal cycle (Shi et al., 2011); the fresh water flux (FWF) from the Changjiang diluted water is found to contain spring-neap signals, too (it is usually maximized during the spring tide) [13, 14]; and, more importantly, there has been evidence that the spring-neap cycles may potentially affect the YSCWM in fall [15]. However, there has been rare attention to the influence of the spring-neap cycle on the generation and evolution of the SCPs. The study as of today is Huang et al. [16], which will be briefly summarized here. In the following, we first give a brief description of the seasonal evolution of the SCPs (Section 2) and then set up a three-dimensional (3D) model to test the hypothesis (Section 3). Section 4 provides a validation of the results. Based on the model results, Section 5 gives a detailed analysis of the effects of the spring-neap tidal cycles on the SCPs. This article is summarized in Section 6.

2. The observed seasonal SCP evolution

Figure 2 shows the seasonal evolution of the Yellow Sea SCPs with the multi-year Moderate Resolution Imaging Spectroradiometer (MODIS) SST data (2003–2016). As can be seen, the

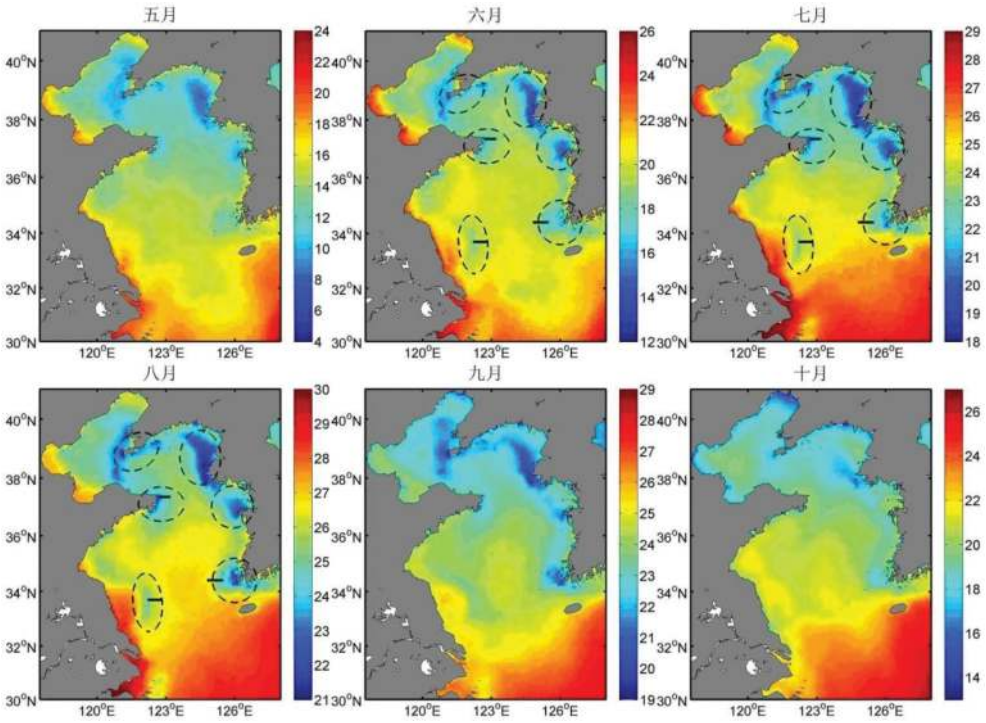

Figure 2. Monthly SST (in °C) climatology (2003–2016) based on MODIS-Aqua and -Terra measurements from May to October. The SCPs are marked by dashed ellipses during summer time and the three lines are shown in the June map.

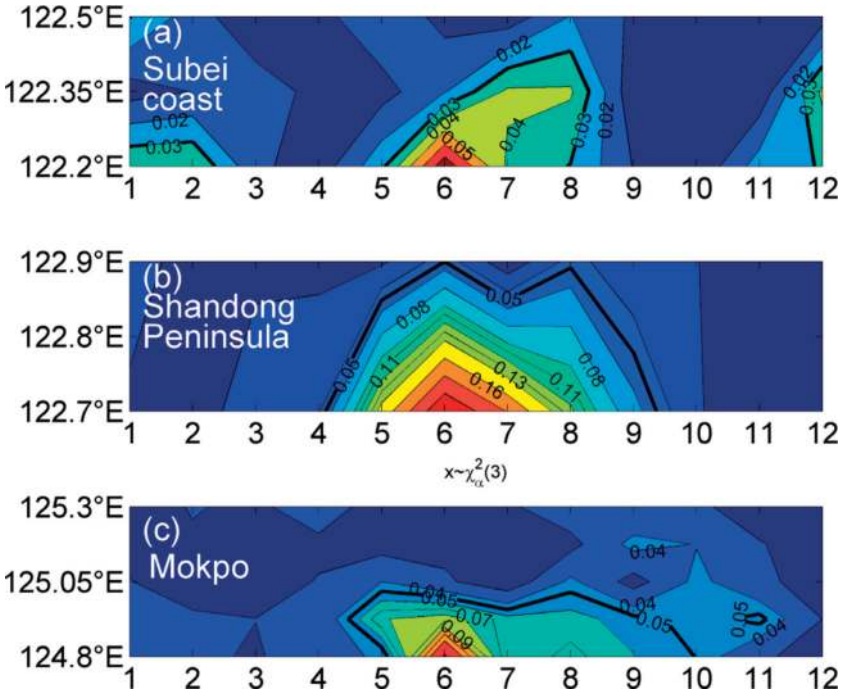

Figure 3. Annual cycles of the $|S_T|$ (from MODIS) off (a) Subei coast (122.2°E–122.5°E, 33.7°N), (b) Shandong Peninsula (122.7°E–122.9°E, 37.35°N), and (c) Mokpo (124.8°E–125.3°E, 34.4°N). Units are K/km.

SCPs usually appear in spring and decay in fall and become pronounced in summer. For a better illustration, we follow Ma et al. [17] and compute the zonal temperature gradient $S_T = \frac{\partial T}{\partial X}$ and display in **Figure 3** $|S_T|$ for the segments off Subei coast, Shandong Peninsula, and Mokpo (the three lines are marked in **Figure 2**). The annual cycles of $|S_T|$ are obvious. Defining the 0.03°C/km isoline as the boundary of the SCP off Subei coast, we then see that the SCP first emerges in May, flourishes in summer, and disappears in late August. Likewise, by defining the 0.05°C/km contour as the boundary, we can have the evolution of the Shandong SCP (**Figure 3b**), which is by observation stronger than its Subei counterpart. It forms in late April, and lasts through late September, with its maximum in June and July. The Mokpo SCP can also be demarcated by the isoline of 0.05°C/km. It is found to emerge in May, lasting through October until it completely disappears.

3. Model setup

We adopt the ECOM-si model developed at *East China Normal University* [14] to achieve our goal. The model domain encompasses the entire East China Sea (including Yellow Sea, Bohai

Sea, and East Sea) and parts of the Pacific Ocean and the Japan Sea, with an open boundary roughly parallel to the Ryukyu Islands. This model has a resolution varying from several hundred meters near the Changjiang River mouth to 2–3 km in the open ocean. Vertically there are 20 terrain-following sigma levels. Besides, a wet/dry scheme is included with a critical depth of 0.25 m. Wu et al. [18] found that the inclusion of inter-tidal flats is very important in simulating the Changjiang plume.

The open boundary conditions include specified shelf and tidal currents. The former is extracted from the daily Hybrid Coordinate Ocean Model (HYCOM) data with a horizontal resolution of 1/12°, the latter is specified with harmonic constants as determined by Wu et al. [13]. The boundary and initial conditions of salinity and temperature are extracted from the daily HYCOM and Simple Ocean Data Assimilation (SODA) datasets, respectively, and the surface fluxes (heat and momentum fluxes) are derived from the European Centre for Medium-Range Weather Forecasts (ECMWF) dataset (with a time resolution of 6 hours). For more details, see Wu et al. [13, 14].

The integration begins on January 1, 2008. After 1 year's spin-up, the model reaches a statistical equilibrium. In the following, the hourly outputs for the summer time (July–August) from 2009 to 2013 will be used.

4. Validation

4.1. Temperature

Our focus is the summertime SCPs, so we look only at simulation for July and August. Data used for validation span an extended multi-year period from 2009 to 2013.

We first compare the model results with historical in situ observations. **Figure 4** shows such a comparison between the cruise data from Korean Oceanographic Data Center (KODC) and

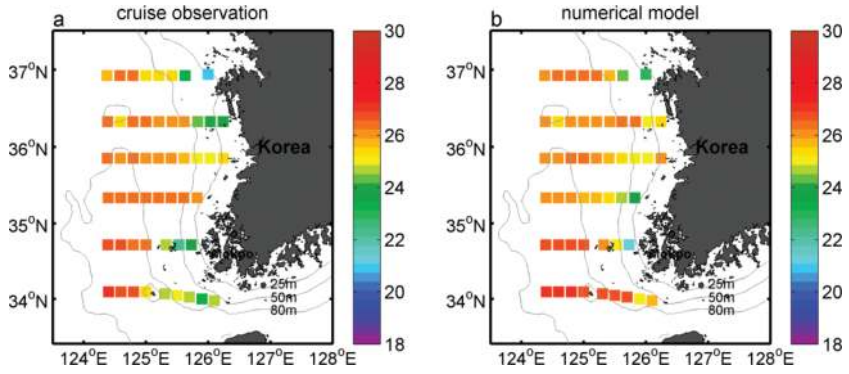

Figure 4. (a) KODC hydrographic mean SST in summer time from 2010 to 2013 (22 Aug 2010–27 Aug 2010; 1 Jul 2011–5 Jul 2011; 10 Aug 2012–18 Aug 2012; 13 Aug 2013–20 Aug 2013). (b) As (a), but for modeled SST. Contours denote the bathymetry of the Yellow Sea (contour interval: 25 m).

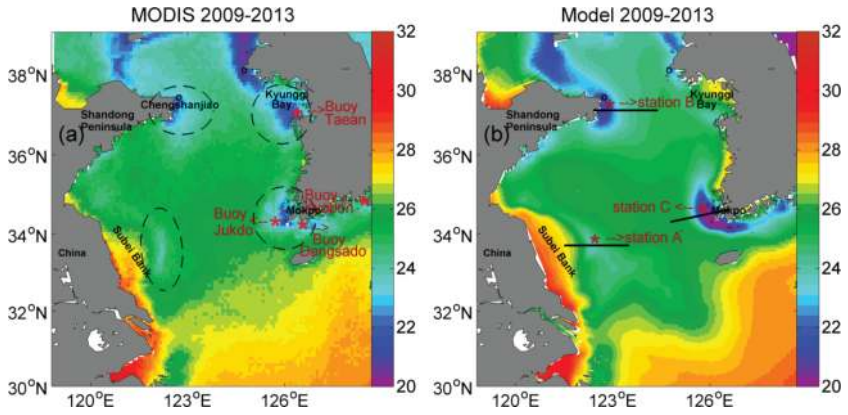

Figure 5. Distribution of the monthly mean SST (°C) from July to August for 2009–2013 from (a) MODIS and (b) model result. The SCPs are marked by dashed ellipses.

National Fishers Research and Development Institute (NFRDI). From it, we see that the simulation has produced satisfactory results comparable with the cruise observations, with an error tolerance within 2°C.

A comparison of the model results with the MODIS also shows good agreement. **Figure 5a** and **b** are the observed (MODIS) and modeled monthly mean SST from July to August, respectively. Generally, the latter agrees well with the former, although the modeled SST off Subei coast is warmer than the MODIS SST by 1–2°C. From both distributions, four SCPs are evident; they are located off Subei Bank, off Chengshanjiao (Cheng Shan Point in the east of Shandong), in Kyunggi Bay, and off Mokpo. Their intensities are also in good agreement, except for that of the two along the Korean coast. Nonetheless, the simulated Mokpo SCP is still satisfactory, though it is too strong by comparison. The problem is with the Byunggi Bay SCP, which is not well reproduced in the model. This is because (1) the model does not have enough resolution around the bay (data unavailable), and (2) the Han River discharge into the Bay is not included (also due to a lack of data). We have tested with some artificial runoff but it seems that the SCP simulation in the bay is essentially not affected, so the poor bathymetry resolution in the eastern part of the Yellow Sea may be blamed. But, anyhow, our focus will be the SCPs off Subei, Shandong, and Mokpo, which will not be influenced by the unsatisfactory simulation of the SST around the Kyunggi Bay.

4.2. Tides

Tides are pivotal to the SCP formation; their successful simulation is the key to this study. **Figure 6** shows the modeled cotidal charts for the four major constituents M2, S2, K1, O1, N2, and P1. From the semidiurnal tides (M2 and S2), we particularly see two amphidromic points in the Yellow Sea (located off Chengshanjiao and Haizhou Bay). These, among other features, agree well with satellite observations and previous model results such as Fang et al. [19], Lu et al. [8], Ren et al. [11], to name a few. Our model simulation is hence validated.

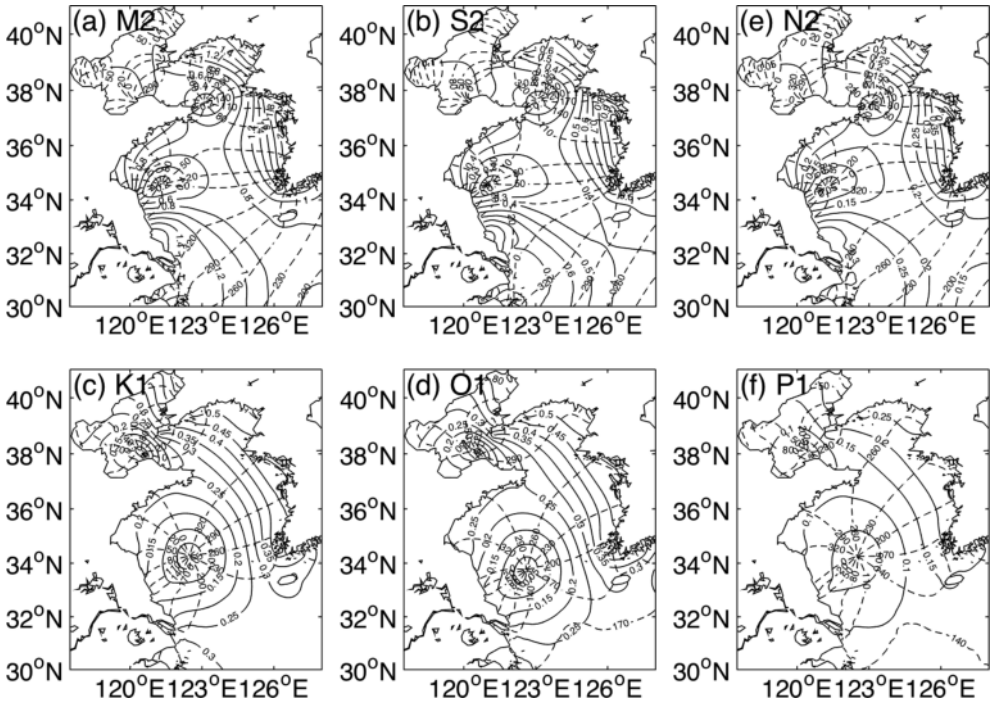

Figure 6. Simulated cotidal charts for (a) M2, (b) S2, (c) K1, (d) O1, (e) N2, and (f) P1 tidal constituents. Dashed and solid lines denote phase lag (degree; referred to Beijing standard time (UTC+8)) and amplitude (cm), respectively.

5. The tidal cycles of the Yellow Sea SCPs

First, look at the evolution of the Subei SCP. For this purpose, a point east of the Subei Bank or Subei Shoal is chosen to plot the time series of the modeled temperature. This is the station A (122.3°E, 33.7°N), as marked in **Figure 5b**. **Figure 7** displays the 3-m temperature (blue) at it from July to August for the 5 years 2009–2013. They are then band-pass filtered with a Butterworth filter to retain only the features between 7 and 21 days and re-plotted in red. Clearly, the spring-neap cycle exists in all the 5 years' band-passed signals—the near surface water is coldest (warmest) during the spring (neap) tidal phases. For the vertical distribution at the station, the cycle is also obvious. **Figure 8** displays the 2012 sequence of the profiles of temperature, vertical velocity, vertical diffusivity, horizontal speed, and the reconstructed tidal current magnitude and surface elevation, from which the spring-neap variations are clearly seen.

The variations of the above oceanic fields provide a possible explanation for the corresponding SCP cycle. During the spring tidal phases, the strong tidal mixing brings up the deep cold water, while the upwelling supplies cold water from the subsurface layer. During the neap tidal phases, the tidal mixing is minimized, and the upwelling in the upper layer is weak. The deep cold water cannot be brought to the surface and, accordingly, the SCP is suppressed. For

http://dx.doi.org/10.5772/intechopen.80732

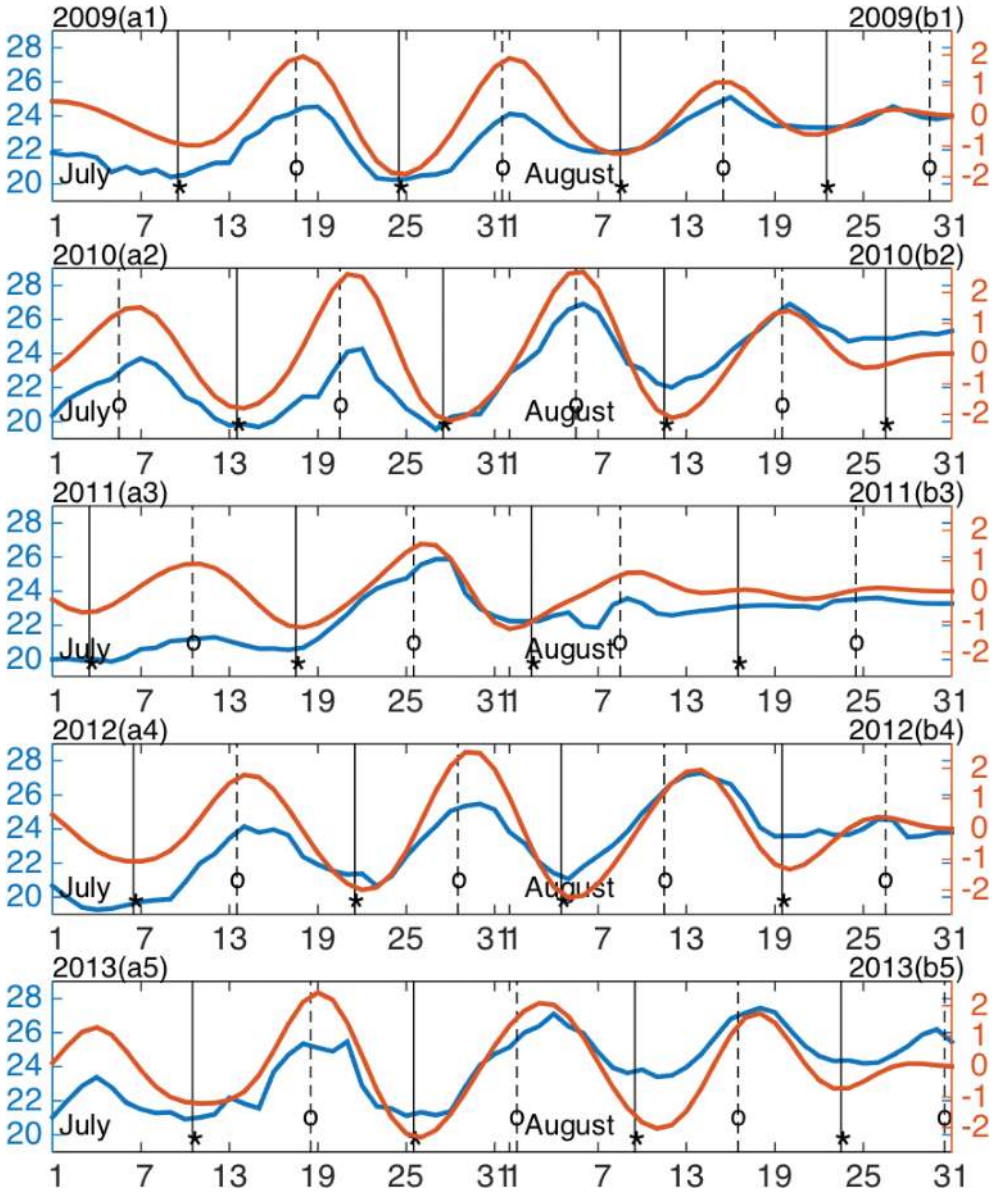

Figure 7. Time series of modeled temperature (°C) at station A from July to August for 2009–2013. Blue: Raw time series; red: band-pass (7–21 days) filtered time series. The asterisk indicates the time of spring tide, while the circle marks that of neap tide.

example, on July 13 (Day 13) and August 12 (Day 43), a strong stratification is established in the absence of mixing and convection; the upper layer water becomes warmer, and hence the SCP fades away.

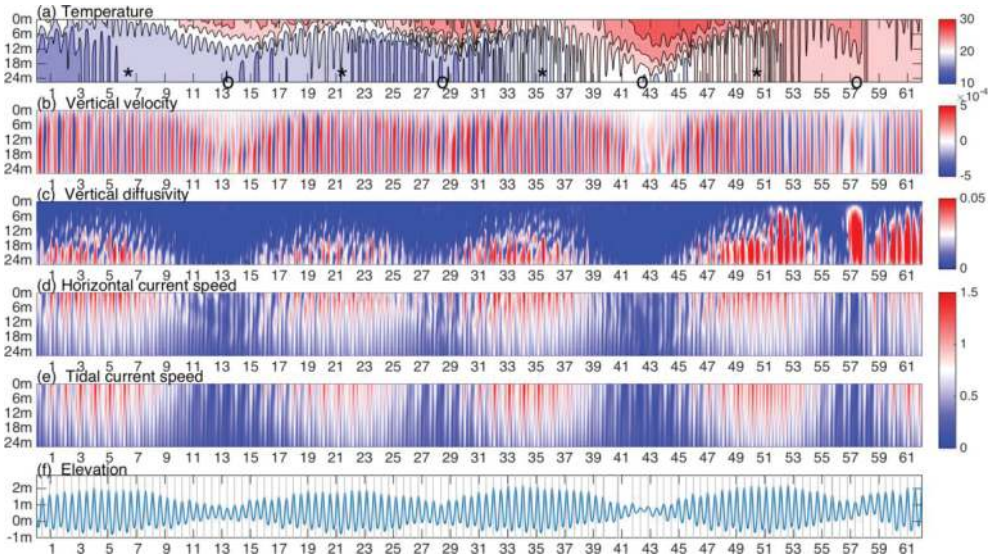

Figure 8. Time-depth distribution of the modeled and reconstructed data at station A (**Figure 5b**) from July to August 2012. The rows from top to bottom are (a) temperature (°C), (b) vertical velocity (ms^{-1}), (c) vertical diffusivity ($m^2\ s^{-1}$), (d) horizontal current (ms^{-1}), (e) reconstructed tidal current velocity (ms^{-1}), and (f) surface elevation (m). The asterisk indicates the time of spring tide, while the circle denotes that of neap tide.

The SCP has a vertical structure which also experiences a variation over the spring-neap tidal cycle. **Figure 9** shows a sequence of the temperature on the cross-section along the latitude 33.7°N, from 121.5°E to 123.5°E in August 2012. From the figure, we see that, on August 4, 2 days after the new moon, the SCP reaches its maximum strength, with the 23°C isotherm line outcropping to the surface. On August 11, just 2 days after the first quarter moon, the outcropping isoline is 26°C, which, however, is completely suppressed during August 12–16. The spring-tide SCP temperature may differ from the neap-tide SCP temperature by as large as 3°C. Obviously, tides along cannot account for all the SCP formation; the effect of the spring-neap tidal variation cannot be ignored.

To contrast the spring tidal temperature from the neap tidal temperature, we, respectively, take the means of the temperatures on the spring tide days (defined as 2 days after new or full moon) and neap tide days (2 days after quarter moon) in summer for all the 5 years during 2009–2013. The mean temperatures are shown in **Figure 10a** and **b**; also shown is their difference (**Figure 10c**). The large difference in both structure and magnitude implies that the previous analysis simply based on the monthly mean fields cannot tell the whole story. Particularly, the large difference in temperature, as shown in **Figure 10c**, happens to take place in the region where the SCP forms, corresponding well to the spring-neap variation. Therefore, for the region off Subei Bank, we may safely say that the formation of the summertime SCP is mainly induced during the spring phase because of the pronounced tidal effect. In the days of

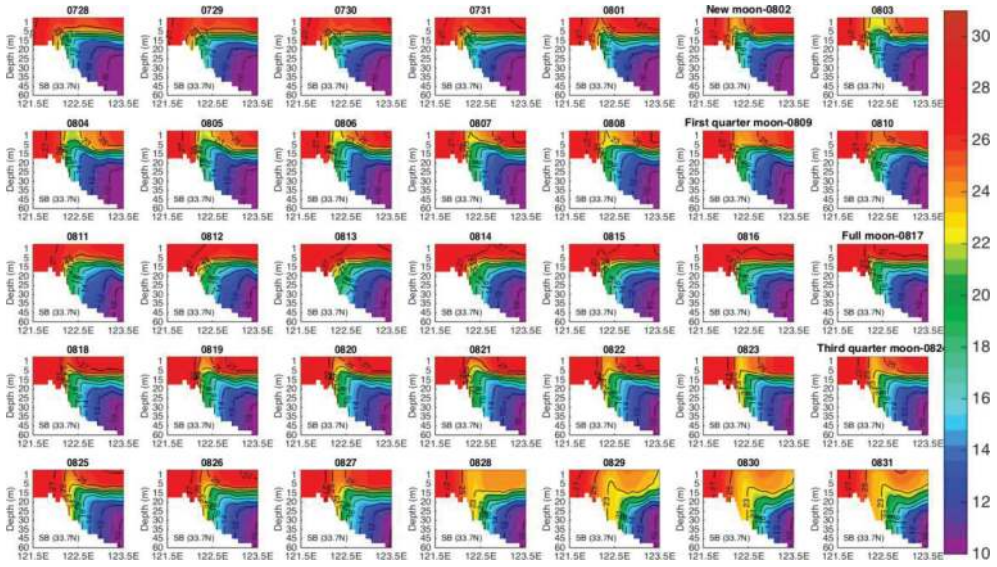

Figure 9. Temperature profiles along 33.7°N from August 1 to August 31. The 22–26°C isolines (with a 1°C interval) are contoured.

neap tides, such as August 14–16, 2012, with the establishment of strong stratification, the weak tidal effect cannot have the deep cold water brought up to the surface, and the SCP may completely be suppressed.

Another conspicuous SCP along the China coast is the one off Shandong Peninsula. Following the same procedure as above, we pick a representative point or "station" B at (122.7°E, 37.1°N), as marked in **Figure 5b**, for the analysis. Shown in **Figure 11** are the original and band-pass filtered temperature series at the point. Compared with that of **Figure 7**, the spring-neap variation at B is much weaker; its maximal magnitude is less than 1°C (~2°C in **Figure 7**). The evolutions of the vertical structures of the fields at B are also distinctly different from those at A, as drawn in **Figure 12**. This is particularly true for the vertical velocity (**Figure 12b**), which is not only weaker than its counterpart at A (off Subei Bank) but also tends to be homogenized over the spring-neap cycle and vertical diffusivity (**Figure 12c**), which implies that the here tidal mixing is strong during the spring phases, and hence the water column tends to be more homogeneously distributed in the vertical direction. It has been reported that tidal mixing plays the dominant role in inducing the Shandong Front [8, 11]. Our results are in agreement with this.

Following what we did in **Figure 10**, we draw the mean temperature profile along the latitude 37.1°N off the tip of Shandong peninsular (marked in **Figure 5b**) for both the spring and neap tidal phases (**Figure 13a** and **b**). What makes a remarkable difference from that in **Figure 10** is the insignificant difference between **Figure 13a** and **b**. In fact, the spring and neap profiles here look quite similar (the difference is shown in **Figure 13c**), in sharp contrast to those off the

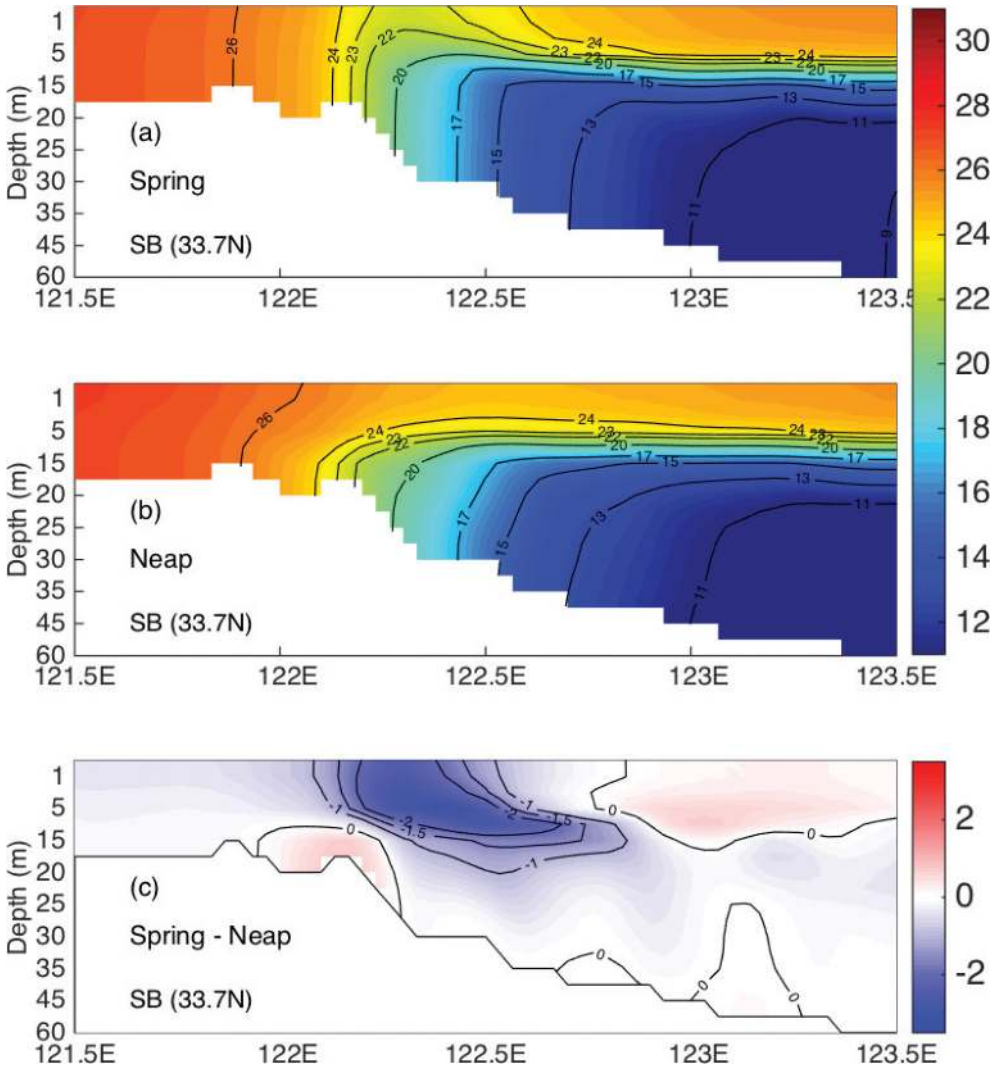

Figure 10. Section profiles of the (a) spring mean, (b) neap mean, and (c) their difference (spring minus neap) temperature along the 33.7°N, from 121.5°E to 123.5°E off the Subei coast.

Subei Bank. By this observation, the previous studies on SCPs using the monthly mean temperature data may be appropriate only for the cold patch off Shandong.

Previously, Ren et al. [11] suggested that tidal mixing is the key to the formation of the Shandong Front, while off Subei Bank, the Subei Front results from collaboration of both tidal

http://dx.doi.org/10.5772/intechopen.80732

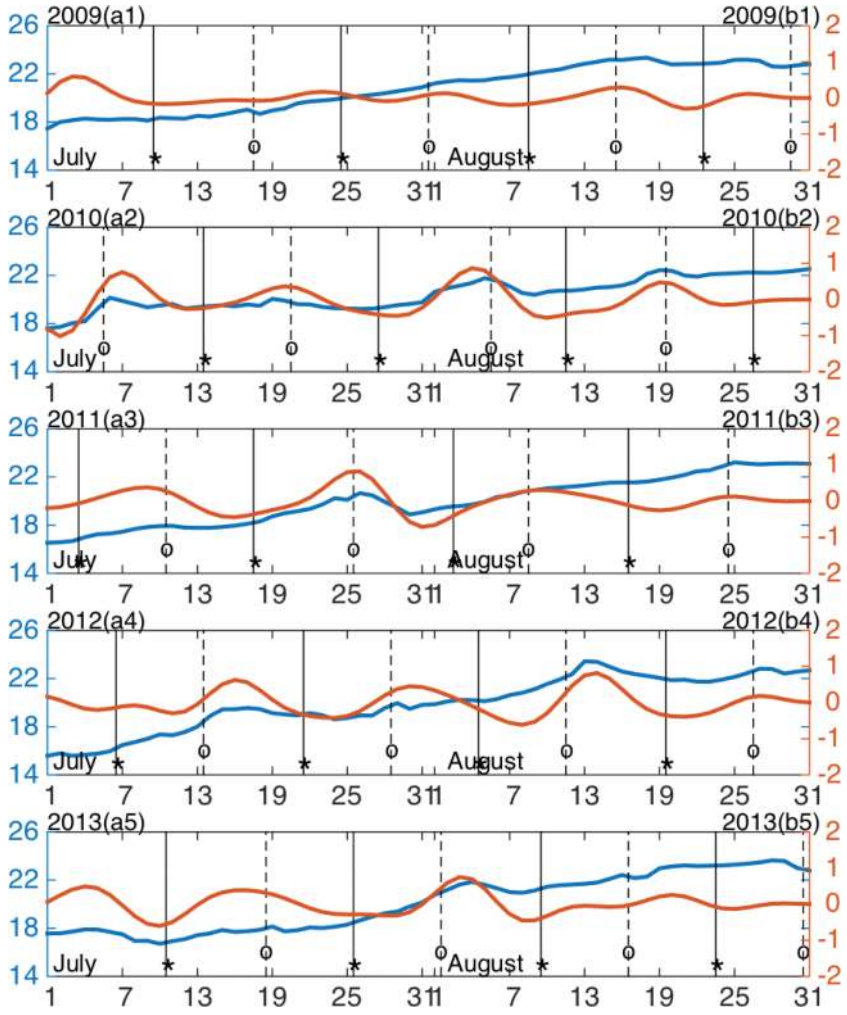

Figure 11. As **Figure 7**, but for station B.

induced upwelling and tidal mixing. The different generating mechanisms may be reflected in the temperature distribution, and hence we see different temperature variations over the spring-neap cycle at the two stations A and B.

The third SCP in the Yellow Sea, the SCP off Mokpo southwest of Korean Peninsula, is somehow different from both its counterparts in the western Yellow Sea. Again, we choose a representative point C at 125.6°E, 34.7°N (cf. **Figure 5b**), and analyze the temperature series at it (**Figure 14**). Similar to station A (off Subei coast), the series at this station also shows

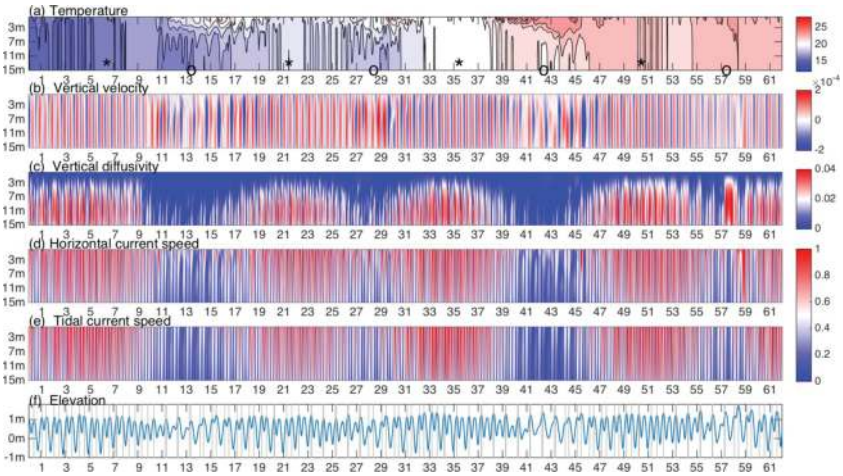

Figure 12. As **Figure 8**, but for station B.

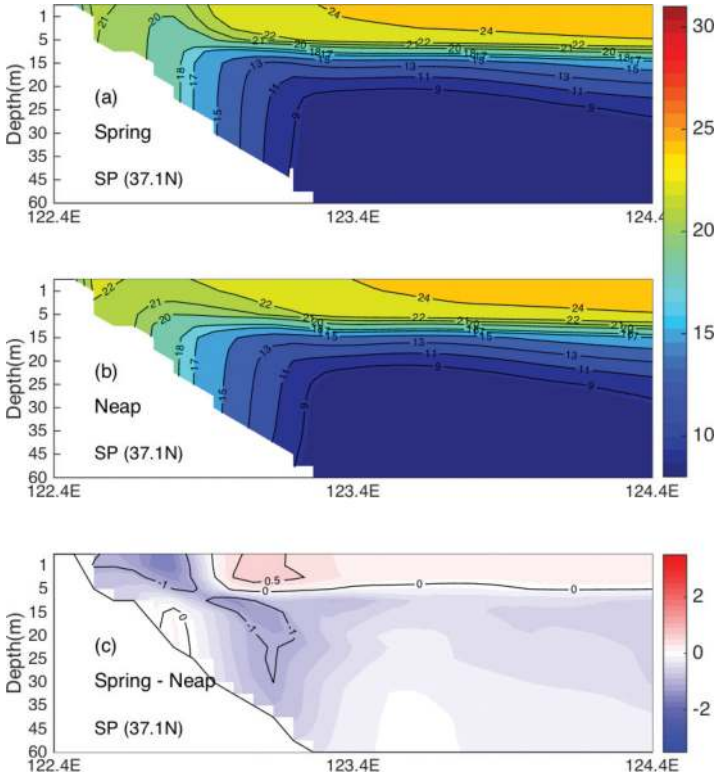

Figure 13. As **Figure 10**, but for the profiles off Shandong Peninsula.

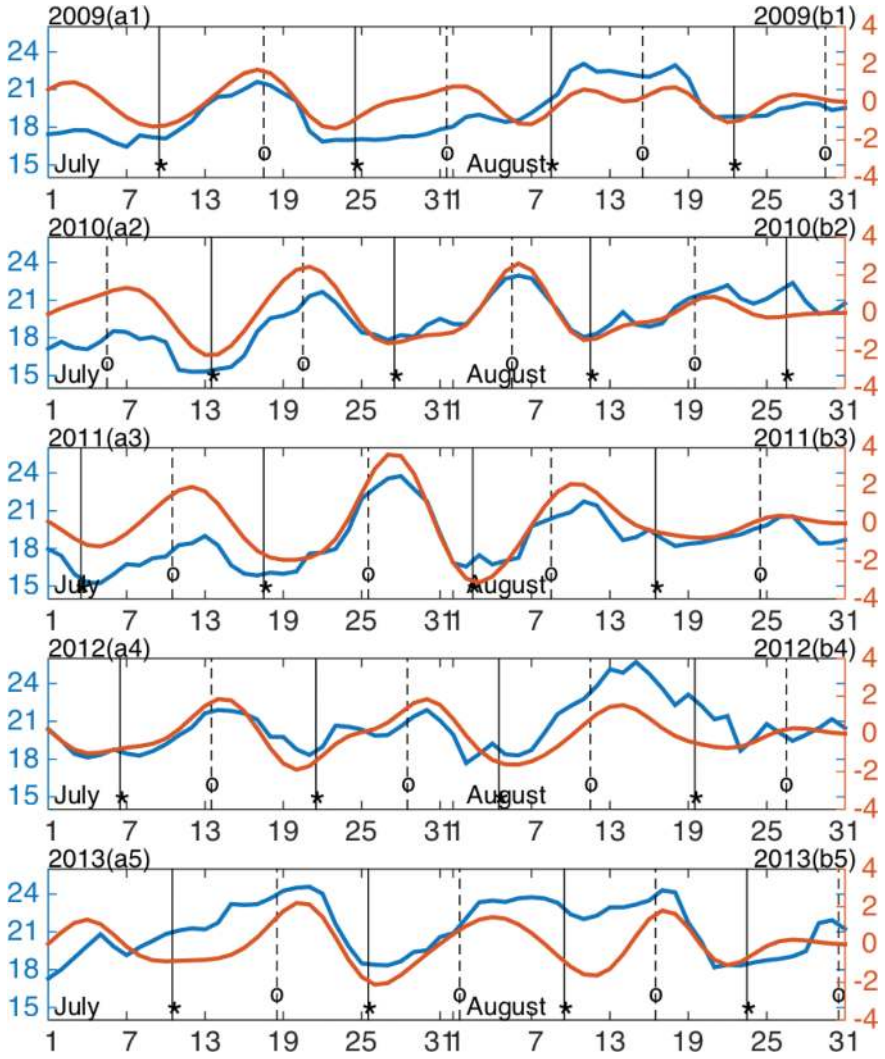

Figure 14. As **Figure 7**, but for station C.

significant spring-neap variations. From **Figure 15**, both upwelling and tidal mixing are conspicuous on the spring-neap cycle. During the spring tidal phases, strong upwelling and strong tidal mixing lead to the generation of the SCP, while during the neap tidal phases, the SCP fades away as both the vertical velocity and vertical diffusivity become greatly weakened.

As we did for **Figure 10**, the cross-section temperature distribution along the latitude ~34.5°N off the tip of Mokpo (marked in **Figure 5b**) is displayed in **Figure 16**. Here, the outcropped isoline on the spring profile is about 19°C, while on the neap profile, it is around 21°C. The

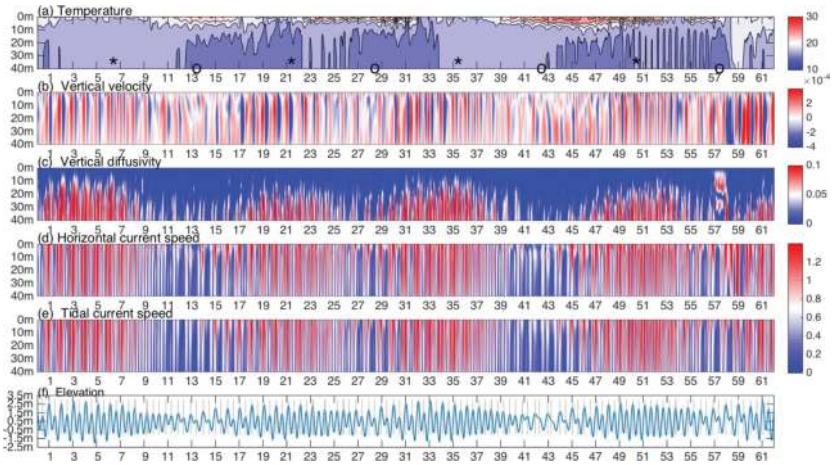

Figure 15. As **Figure 8**, but for station C.

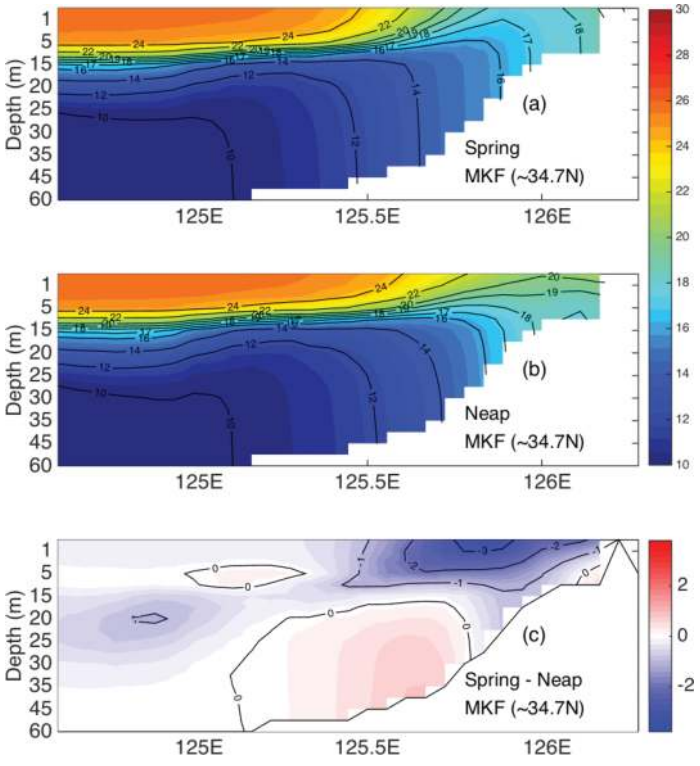

Figure 16. As **Figure 10**, but for the profile off Mokpo.

spring-neap difference (**Figure 16c**) shows a pattern just like that of **Figure 10c**, with a minimum trapped in the near-surface below the SCP and vanishing values elsewhere.

6. Concluding remarks

The long observed SCPs along the China and Korea coasts are a conspicuous hydrographic phenomenon in Yellow Sea. They generally form in spring, grow in summer, and decay in fall, though the precise time may differ case by case. Using a 3D numerical model, in this study, we have investigated how the spring-neap tidal cycle influences the formations and evolutions of these SCPs in July and August.

The temperature variation over a spring-neap tidal cycle separated from the nonstationary background shows that the lowest temperature occurs during spring tidal days (defined as 2 days after new moon or full moon), and the highest occurs during neap tidal days (2 days after quarter moon). This spring-neap variation is consistent with the previous ocean color observation by, say, Shi et al. [20], who showed that the ocean color in Yellow Sea varies on a period largely equivalent to a spring-neap tidal cycle, with the largest (smallest) turbid water coverage 2–3 days behind the new/full (quarter) moon. This variation is the most conspicuous for the SCPs off Subei Bank and off Mokpo, while for the Shandong SCP, it is not significant, suggesting that the underlying generating mechanism could be different. Indeed, the time-depth distributions of temperature, vertical velocity, and vertical diffusivity off Subei Bank show that the mixing is weak, and vertical velocity is small in the neap tidal phase, and, as a result, strong stratification is established, suppressing the upwelling and subsequently the SCP; on the other hand, the SCP is enhanced in the spring phase, thanks to the strong upwelling and tidal mixing which bring the deep cold water upward through the thermocline to the surface. The Mokpo SCP bears a similar variable scenario. The Shandong SCP, however, does not show significant variation over a spring-neap cycle. Its formation is mainly through tidal mixing, in contrast to the Subei SCP and Mokpo SCP. But here the tidal mixing alone makes a relatively homogeneous temperature distribution in the vertical direction. This prevents the influence of the spring-neap cycle from taking effect on the vertical movement of deep water, yielding an insignificant spring-neap variation. The composite analysis of the MODIS SST data and buoy observations also support these observations.

Acknowledgements

The hydrography and buoy data are from the Korean Oceanographic Data Center (KODC; http://kodc.nifs.go.kr/page?id=kr_index) and National Marine Data and Information Service (NMDIS; http://www.cmoc-china.cn/). The MODIS data are available at (https://modis.gsfc.nasa.gov/), and the phases of the moon are provided by NASA (https://eclipse.gsfc.nasa.gov/lunar.html). The surface fluxes are from ECMWF (http://apps.ecmwf.int/datasets/). This study was partially supported by the 2015 Innovation Program for Research and Entrepreneurship Teams, Jiangsu, China.

Author details

X. San Liang[1,2]*, Minghai Huang[1], Hui Wu[3] and Yihe Wang[3]

*Address all correspondence to: x.san.liang@gmail.com

1 School of Marine Sciences, Nanjing University of Information Science and Technology, Nanjing, China

2 School of Atmospheric Sciences, Nanjing University of Information Science and Technology, Nanjing, China

3 State Key Laboratory of Estuarine and Coastal Research, East China Normal University, Shanghai, PR China

References

[1] Uda M. The results of simultaneous oceanographical investigations in the Japan Sea and its adjacent waters in May and June 1932. Journal of the Imperial Fishery Experimental Stations (In Japanese). 1934;(5):57-190

[2] Feng M, Hu D, Li Y. A theoretical solution for the thermohaline circulation in the Southern Yellow Sea. Chinese Journal of Oceanology and Limnology. 1992;**10**(4):289-300

[3] Li H, Yuan Y. On the formation and maintenance mechanisms of the cold water mass of the Yellow Sea. Chinese Journal of Oceanology and Limnology. 1992;**10**(2):97-106

[4] Su J, Huang D. On the current field associated with the Yellow Sea cold water mass. Chinese Journal of Oceanology and Limnology. 1995;(S1):1-7

[5] Seung Y-H, Chung J-H, Park Y-C. Oceanographic studies related to the tidal front in the mid-Yellow Sea off Korea: Physical aspect. Journal of the Oceanological Society of Korea. 1990;**25**:84-95

[6] Zou EM, Guo BH, Tang YX, Lee JH, Lie HJ. An analysis of summer hydrographic features and circulation in the Southern Yellow Sea and the Northern East China Sea. Oceanologia et Limnologia Sinica. 2001;**32**(3):340-348

[7] Lie HJ. Summertime hydrographic features in the Southeastern Hwanghae. Progress in Oceanography. 1986;**17**(17):229-242

[8] Lü X, Qiao F, Xia C, Wang G, Yuan Y. Upwelling and surface cold patches in the yellow sea in summer: Effects of tidal mixing on the vertical circulation. Continental Shelf Research. 2010;**30**(6):620-632

[9] Zhao B. A preliminary study of continental shelf fronts in the western part of southern Huanghai sea and circulation structure in the front region of the Huanghai cold water

mass (HCWM). Oceanologia et Limnologia Sinica. 1987 (in Chinese, with English Abstr); **18**:217-226

[10] Simpson JH, Hunter JR. Fronts in the Irish Sea. Nature. 1974;**250**(5465):404-406

[11] Ren S, Xie J, Jiang Z. The roles of different mechanisms related to the tide-induced fronts in the Yellow Sea in summer. Advances in Atmospheric Sciences. 2014;**31**(5):1079-1089

[12] Li M, Zhong L. Flood–ebb and spring–neap variations of mixing, stratification and circulation in Chesapeake Bay. Continental Shelf Research. 2007;**29**(1):4-14

[13] Wu H, Zhu J, Shen J, Wang H. Tidal modulation on the Changjiang River plume in summer. Journal of Geophysical Research – Atmospheres. 2011;**116**(C8):192-197

[14] Wu H, Shen J, Zhu J, Zhang J, Li L. Characteristics of the Changjiang plume and its extension along the Jiangsu coast. Continental Shelf Research. 2014;**76**(2):108-123

[15] Li J, Li G, Xu J, Dong P, Qiao L, Liu S, et al. Seasonal evolution of the Yellow Sea cold water mass and its interactions with ambient hydrodynamic system. Journal of Geophysical Research, Oceans. 2016;**121**:6779-6792

[16] Huang M, Liang XS, Wu H, Wang Y. Different generating mechanisms for the summer surface cold patches in the Yellow Sea. Atmosphere-Ocean. 2017:1-13. DOI: 10.1080/07055900.2017.1371580

[17] Ma J, Qiao F, Xia C. Tidal effects on temperature front in the Yellow Sea. Chinese Journal of Oceanology and Limnology. 2004;**22**(3):314-321

[18] Wu H, Zhu J. Advection scheme with 3rd high-order spatial interpolation at the middle temporal level and its application to saltwater intrusion in the Changjiang estuary. Ocean Modelling. 2010;**33**(1–2):33-51

[19] Fang G, Wang Y, Wei Z, Choi BH, Wang X, Wang J. Empirical cotidal charts of the bohai, yellow, and east china seas from 10 years of topex/poseidon altimetry. Journal of Geophysical Research – Atmospheres. 2004;**109**(C11):227-251

[20] Shi W, Wang M, Jiang L. Spring–neap tidal effects on satellite ocean color observations in the Bohai Sea, Yellow Sea, and East China Sea. Journal of Geophysical Research – Atmospheres. 2011;**116**(C12032). DOI: 10.1029/2011JC007234